Phys. Status Solidi A **212,** No. 4, 846–850 (2015) / **DOI** 10.1002/pssa.201431779

physica status solidi pss a
www.pss-a.com
applications and materials science

Nitrogen-doped ZnO obtained by nitrogen plasma treatment

Dengkui Wang[1,2], Dongxu Zhao[*,1], Fei Wang[1,2], Bin Yao[3], and Dezhen Shen[1]

[1] State Key Laboratory of Luminescence and Applications, Changchun Institute of Optics, Fine Mechanics and Physics, Chinese Academy of Sciences, 3888 Dongnanhu Road, Changchun 130021, P. R. China
[2] Graduate School of the Chinese Academy of Sciences, Beijing 100049, P. R. China
[3] Department of Physics, Jilin University, Changchun 130023, P. R. China

Received 8 October 2014, revised 24 December 2014, accepted 30 December 2014
Published online 4 February 2015

Keywords nitrogen plasma treatment, photoluminescence, single crystals, work function, zinc oxide

[*] Corresponding author: e-mail: zhaodx@ciomp.ac.cn, Phone: +86-431-86708227, Fax: +86-431-86176312

We carried out a nitrogen plasma treatment process to obtain N-doped ZnO single crystal. The treated sample showed an acceptor related emission located at 3.354 eV when excited by a 325-nm He–Cd laser at 85 K. Raman spectra revealed the formation of a bond between Zn and N atoms. The surface work function indicated increasing of hole concentration of the N-plasma-treated ZnO. By constructing a ZnO-based homojunction, the *I*–*V* curve displayed perfect rectification performance.

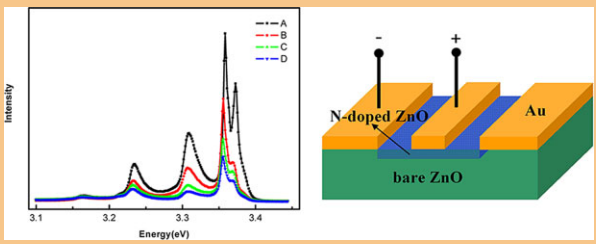

1 Introduction ZnO has always been considered as a potential material for highly efficient ultraviolet optoelectronic devices, such as light-emitting diodes, laser diodes and ultraviolet photodetectors [1–3]. ZnO has a direct wide bandgap with 3.37 eV. Compared with GaN (25 meV) and ZnS (38 meV), it has a larger exciton binding energy of 60 meV, which is far higher than the thermal energy. This can lead to exciton recombination emission at room temperature. Therefore, ZnO is more suitable for ultraviolet optoelectronics than other wide-bandgap semiconductors. In recent years, many scientists have made great progress on the research of room-temperature electroluminescence of ZnO-based homojunction and heterojunction devices [4, 5]. But there is a long way to go before the practical application.

Due to a large number of native defects, such as the oxygen vacancy and zinc interstitial atom, ZnO often shows an n-type character [6–8]. Native defects lead to deep donor levels and strong self-compensation effect. So, the preparation of p-type ZnO is difficult. In order to obtain stable p-type ZnO, the self-compensation effect should be offset by introducing other impurity elements. Nitrogen has a similar atom radius and fewer electrons than oxygen, which is considered as the most promising dopant for p-type ZnO doping. Herein, many groups have prepared p-type ZnO by nitrogen doping [9, 10]. Kawasaki and co-workers [11] reported the achievement of N-doped ZnO by molecular beam epitaxy (MBE) on $ScAlMgO_4$ and ZnO substrates.

Usually, N plasma is used as the activated source during the ZnO doping process. In our previous works, we have carried out the method of doping during deposition process to obtain N-doped ZnO [12]. Chen et al. [12] fabricated N-doped ZnO thin film via plasma-assisted molecular beam epitaxy. In this paper, we utilized a plasma-treatment process to prepare N-doped ZnO single crystal at room temperature. Several studies concerning the effects of ammonia or hydrogen plasma post-treatment on ZnO could be found in the literature [13, 14]. This is the first report of the nitrogen plasma post-treatment on ZnO single crystal. Compared with other methods, nitrogen plasma treatment does not require complex equipment and avoids high fabrication temperatures. Low-temperature photoluminescence and Raman scattering spectra were employed to study luminescence mechanism and determine the nitrogen atom's role in the zinc oxide crystal lattice. The surface work function was applied to study the Fermi energy level

change of the N-doped ZnO single crystal. The current–voltage properties of N-doped ZnO were characterized by using a Keithley 2611 A at room temperature.

2 Experimental The ZnO single crystal used in our experiment was bought from Hefei KeJing Materials Co. Ltd. The carrier density of this crystal was 5.56×10^{16} cm^{-3} and its Hall mobility was 183 cm^2/V s with n-type conductivity. The crystal was cut into pieces of 2.5 mm $\times$ 5 mm. Half of the sample was covered with gold, which was deposited by an electron beam evaporation method. Au could be used not only as an electrode, but also a barrier to obtain ZnO with partial treatment by the nitrogen plasma. Then, the pieces of ZnO were put into a plasma cleaner chamber. We employed high-purity nitrogen (5N) as the gas source to produce a nitrogen plasma under 5 Pa. The plasma treatment was conducted under a voltage of 720 V, a current of 25 mA and a power of 18 W, respectively. As shown in Fig. 1, the N plasma spectrum consisted of three parts, which originated from N_2 molecule (N_2*) (first positive (1st) and second positive (2nd)) and N atom (N*), respectively. But the N* was dominant for N plasma. The samples with treatment for 20 h, 30 h and 40 h at room temperature were labelled as B, C and D, respectively. The sample without the treatment was labelled as A.

The room- and low-temperature photoluminescence spectra measurements were carried out by using a He–Cd laser and a micro-Raman spectrometer. The emission line of the He–Cd laser was 325 nm. The Raman scattering spectrum was measured by using a 488-nm argon ion laser as excitation source and a micro-Raman spectrometer at room temperature. Chemical bonding states of the films were measured by X-ray photoelectron spectroscopy. The work function of the ZnO single crystal surface was assessed with a Kelvin probe. The current–voltage (I–V) characteristic curve of the device was measured by a Keithley 2611 A measurement system.

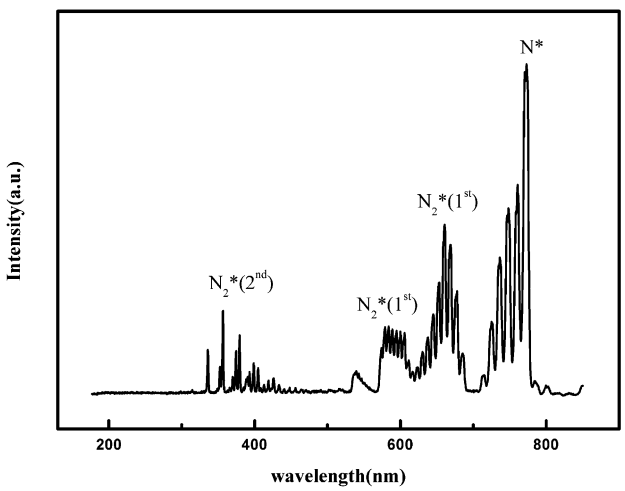

Figure 1 Nitrogen plasma spectra at room temperature.

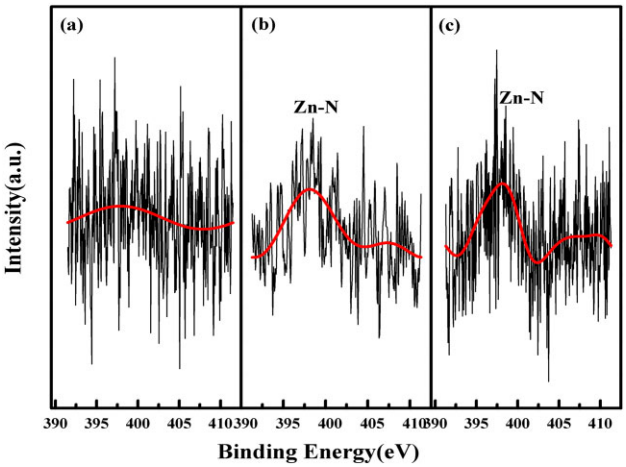

Figure 2 The N_{1s} XPS spectra of different samples. (a) B, (b) C, and (c) D.

3 Results and discussion The XPS is applied to measure the chemical state of N-doped ZnO crystals. Figure 2 is the XPS spectra of different samples. The spectra of sample C and D all show a peak located at 398.2 eV. We attribute this to Zn–N bonding [15]. The appearance of the 398.2 eV peaks confirms the replacement of O atoms with N atoms in the nitrogen plasma treatment ZnO crystal.

Photoluminescence (PL) spectra of different samples at room temperature are shown in Fig. 3a. A strong emission peak around 3.26 eV is observed for undoped and doped (sample D) ZnO. In order to further verify the origin of ultraviolet emission in N-doped ZnO, the low-temperature photoluminescence (LTPL) spectra were measured. The insert in Fig. 3b shows LTPL spectra of ZnO single crystal and the N-doped ZnO single crystals at the liquid-nitrogen temperature. The defect emission is suppressed after N plasma treatment. Figure 3b shows an enlarged figure of the LTPL spectra from 3.1 eV to 3.45 eV. For the bare ZnO single crystal, the free exciton (FX) peak is observed at 3.372 eV. The emission peak at 3.358 eV is attributed to the shallow donor-related bound exciton (D^0X). The three peaks below 3.5 eV are the longitudinal optical (LO)-phonon replicas of the FX, which were assigned to FX-1LO, FX-2LO and FX-3LO. The energy separation between adjacent peaks is about 70 meV. In the N-doped ZnO LTPL spectra, the FX peak intensity decreases with the increase of treatment time and the peak position does not change. This decrease is derived from the N atom in the ZnO lattice. The photon emission at 3.358 eV shifts to 3.354 eV, which is supposed to an acceptor-related bound exciton (A^0X) emission [16]. Nitrogen atoms replace the oxygen atoms at lattice point when introducing the nitrogen element into ZnO single crystal, so a new acceptor energy level will be formed above the valence-band edge. Compared with N replacement O, interstitial N or O defects have higher chemical potential and instability. The possibility of the presence of interstitial N or O defects is ruled out. When the

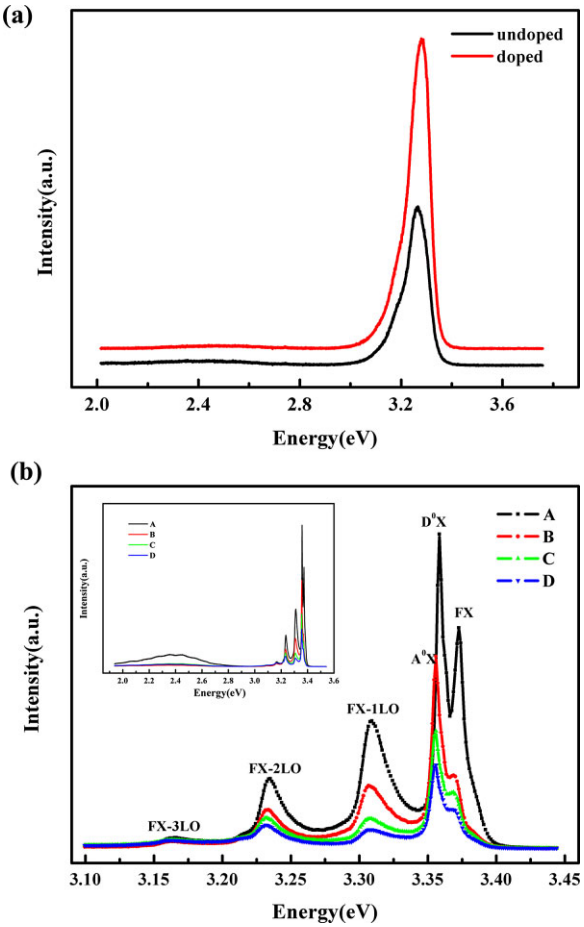

Figure 3 (a) Room-temperature PL spectra of N-doped ZnO (sample D) and undoped ZnO. (b) Low-temperature PL spectra of pure ZnO crystal (A) and N-doped ZnO samples with different treatment time: 20 h (B), 30 h (C) and 40 h (D). The inset is the whole LTPL from 1.8 eV to 3.6 eV.

excited electrons recombine with the holes that lie in the nitrogen acceptor energy level, photon emission will be obtained and the photon energy is less than the bandgap. Therefore, we attribute the peak around 3.354 eV to the shallow acceptor.

To confirm whether the N atoms were doped in ZnO single crystal, Raman scattering was applied. Figure 4 shows the Raman spectra of ZnO single crystal and N-doped ZnO with different treatment times. Usually, ZnO Raman active zone-centre optical phonons consist of A_1, $2E_2$ and E_1 [17, 18]. The phonons of A_1 and E_1 exhibit different frequencies for the transverse-optical (TO) and longitudinal-optical (LO) phonons because of their polar nature. Nonpolar phonon mode E_2 has two frequencies. E_2 (high) is associated with oxygen atoms and E_2 (low) is associated with Zn sublattice. In all samples, we could find five peaks clearly around 96, 200, 329, 435 and 573 cm^{-1}. The Raman modes around 96 and 435 cm^{-1} are considered as E_2 (low) and E_2 (high) [19–21]. It can be concluded that the peaks around 573 cm^{-1} in all samples correspond to A_1(LO). The

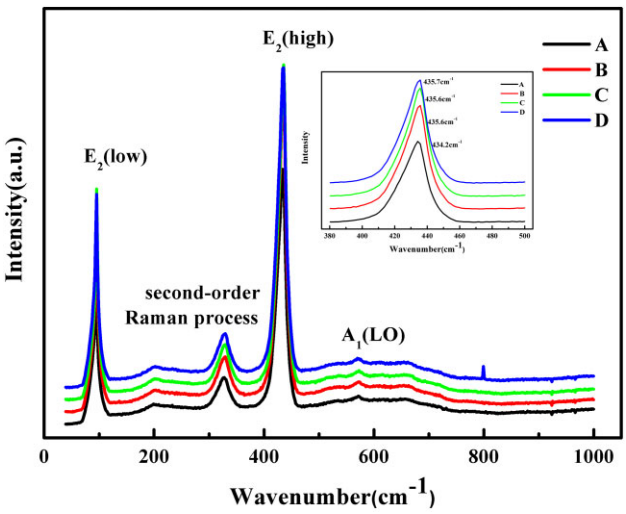

Figure 4 Room-temperature Raman spectra of the four N-doped ZnO samples with treatment time: 0 h (A), 20 h (B), 30 h (C) and 40 h (D). The insert zoom is from 400 cm^{-1} to 500 cm^{-1}.

peak located 329 cm^{-1} is related to the second-order Raman process. Although all Raman spectra are almost the same, they have some subtle differences. As shown in the insert of Fig. 4, the peak position of E_2 (high) shifts to the large wave number side for the samples with longer treatment time [22].

The addition of N atoms to ZnO can cause the appearance of the localized vibration modes (LVM) [22–26]. The LVM frequencies can be estimated using a simple function [27]:

$$\omega_{\mathrm{VLM}} = \omega_{\mathrm{O}} \sqrt{\frac{\mu_{\mathrm{o}}}{\mu_{\mathrm{N}}}}, \tag{1}$$

where μ_{O} ($\mu_{\mathrm{O}} = 16$) and μ_{N} ($\mu_{\mathrm{N}} = 14$) are the relative atomic masses of O and N atoms, respectively. ω_{O} is the vibration mode of O atom. We can conclude the ω_{LVM} value equals up to $1.07\omega_{\mathrm{O}}$ through the equation. The estimated value of the LVM frequency of the N atom is larger than the O atom, leading the wave number of E_2 (high) to become large.

The work function is the minimum energy that is needed to remove an electron from a solid to a point outside the solid surface immediately or to move an electron from the Fermi level into vacuum [28]. The relation between work function and Fermi energy level is given in the following equation:

$$W = -e\Phi - E_{\mathrm{F}}, \tag{2}$$

where $-e$ is the charge of an electron, Φ is the electrostatic potential in the vacuum nearby the surface, and E_{F} is the Fermi level of the semiconductor.

There is a correlation between the change of work function and the movement of the Femi level. By considering the relationship between the Femi level and the ratio of holes and electrons, we can obtain the change of

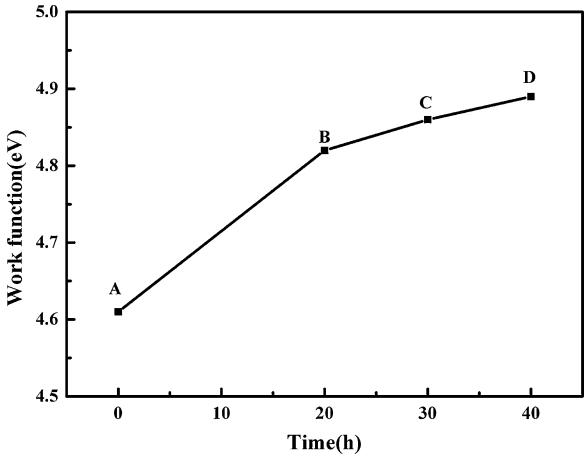

Figure 5 The work function of pure ZnO single crystal (A) and N-doped ZnO samples (20 h (B), 30 h (C) and 40 h (D)).

carrier density by measuring the work function. We measure the work functions of four samples and the results are shown in Fig. 5. The pure ZnO single-crystal work function is 4.61 eV, while other samples have lower levels with the increase of the treatment time. The increase of work function means that the electron concentration decreases or the density of holes increases in ZnO [29]. After N-plasma treatment, N atoms will form an acceptor level in ZnO. This results in the increase of holes concentration and the Fermi level moves close to the valence band. The work function will become larger. The experimental results are consistent with our theory.

From the above experiments, it could be concluded that the N atom could be doped into the ZnO single crystal to generate an acceptor-related energy lever through the N plasma treatment progress. To further understand the conductivity property of the N-doped ZnO, we designed a homojunction device using ZnO single crystal with Au as electrodes. Before verifying the rectification characteristic of the device, we must ensure the contacts of ZnO with Au electrodes are Ohmic. Two Au electrodes were evaporated on the ZnO single crystal surface before and after N plasma treatment (sample D). The *I–V* curves are shown in Fig. 6a. In this device, the ZnO single is treated for 40 h, its surface work function is 4.9 eV. This result matches well with the work function of Au, which is 5.1 eV. The linear curves of Au on bare ZnO and N-doped ZnO reveals that good Ohmic contacts have been obtained in the devices.

The schematic structure of the ZnO homojunction is shown in the insert of Fig. 6b. A gold electrode is deposited on the part of the ZnO with N-plasma treatment via an electron beam evaporation method. The area of electrodes on the surface of pure ZnO and N-doped ZnO is 2.5 mm × 1 mm. The thickness of electrodes is 120 nm. The distance between the Au electrodes is 1 mm. To study the conduction performance of the treated samples, the device was produced using sample D. The current-voltage

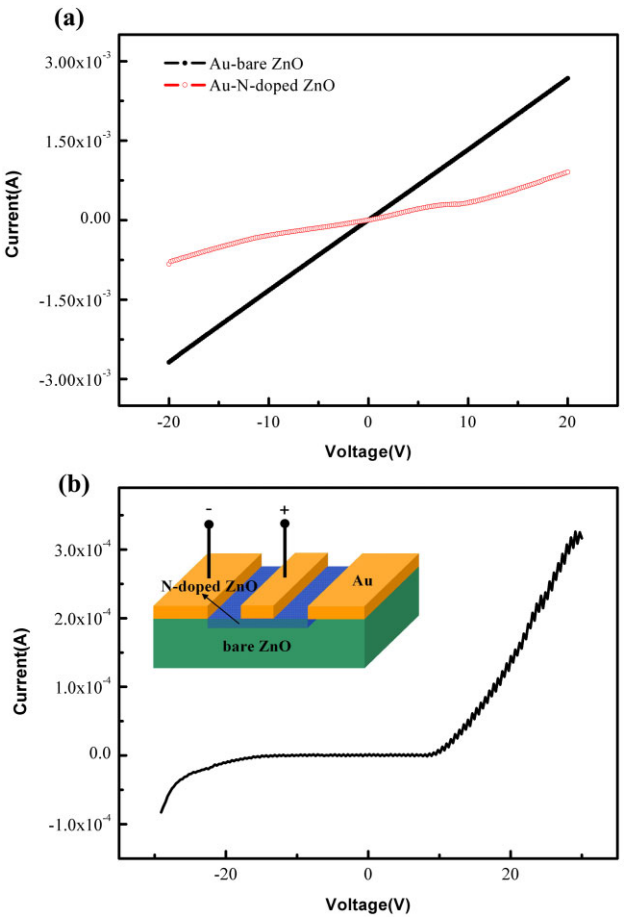

Figure 6 (a) The *I–V* characteristic curves for Au on bare ZnO and N-doped ZnO (sample D). (b) The *I–V* characteristic curve of the ZnO homojunction device at room temperature. The inset is the schematic structure of the ZnO homojunction device.

measurement is performed at room temperature and the result is shown in Fig. 6b. The result also proves the existence of a homojunction between the treatment part and original part. As expected, the *I–V* curve of the device displays perfect rectification performance with the threshold voltage of about 8 V. The threshold voltage is higher than the bandgap of ZnO, owing to the high resistivity of the N-doped ZnO layer. Similar results have been reported by others [11].

4 Conclusions In summary, N-doped ZnO was achieved via N-plasma-treatment processing. In the plasma atmosphere, the nitrogen atom and zinc oxide had a collision reaction, thus the nitrogen atom could substitute oxygen atom in the ZnO single crystal. The doping of nitrogen atom in ZnO was realized. By the measurement of LTPL, Raman scattering spectra and surface work function, it could be confirmed that the N was successfully doped into ZnO. We found a new method to realize the nitrogen doping of ZnO by N-plasma treatment.

Acknowledgements This work was supported by the National Basic Research Program of China (973 Program) under Grant No. 2011CB302004, the Key Program of National Natural Science Foundation of China under Grant No. 11134009, the National Natural Science Foundation of China under Grant Nos. 11074248, 11104265, 21101146.

References

[1] Y. I. Alivov, J. E. Van Nostrand, D. C. Look, M. V. Chukichev, and B. M. Ataev, Appl. Phys. Lett. **83**, 2943 (2003).
[2] X. W. Fu, Z. M. Liao, J. Xu, X. S. Wu, W. L. Guo, and D. P. Yu, Nanoscale **5**, 916 (2013).
[3] C. Soci, A. Zhang, B. Xiang, S. A. Dayeh, D. P. R. Aplin, J. Park, X. Y. Bao, Y. H. Lo, and D. Wang, Nano. Lett. **7**, 1003 (2007).
[4] W. Z. Xu, Z. Z. Ye, Y. J. Zeng, L. P. Zhu, B. H. Zhao, L. Jiang, J. G. Lu, H. P. He, and S. B. Zhang, Appl. Phys. Lett. **88**, 173506 (2006).
[5] M. Willander, O. Nur, S. Zaman, A. Zainelabdin, N. Bano, and I. Hussain, J. Phys. D, Appl. Phys. **44**, 224017 (2011).
[6] D. C. Look, J. W. Hemsky, and J. R. Sizelove, Phys. Rev. Lett. **82**, 25525 (1999).
[7] K. Vanheusden, C. H. Seager, W. L. Warren, D. R. Tallant, and J. A. Voigt, Appl. Phys. Lett. **68**, 403 (1996).
[8] A. Janotti and C. G. Van de Walle, Phys. Rev. B **76**, 165202 (2007).
[9] X. Y. Yang, A. Wolcott, G. M. Wang, A. Sobo, R. C. Fitzmorris, F. Qian, J. Z. Zhang, and Y. Li, Nano Lett. **9**, 2331 (2009).
[10] Y. Zhu, S. S. Lin, Y. Z. Zhang, Z. Z. Ye, Y. F. Lu, J. G. Lu, and B. H. Zhao, Appl. Surf. Sci. **255**, 6201 (2009).
[11] A. Tsukazaki, A. Ohtomo, T. Onuma, M. Ohtani, T. Makino, M. Sumiya, K. Ohtani, S. F. Chichibu, S. Fuke, Y. Segawa, H. Ohno, H. Koinuma, and M. Kawasaki, Nature Mater. **4**, 42 (2005).
[12] X. Y. Chen, Z. Z. Zhang, B. Yao, M. M. Jiang, S. P. Wang, B. H. Li, C. X. Shan, L. Liu, D. X. Zhao, and D. Z. Shen, Appl. Phys. Lett. **99**, 091908 (2011).
[13] R. Huang, S. G. Xu, W. H. Guo, L. Wang, J. Song, T. W. Ng, J. N. Huang, S. T. Lee, S. W. Du, and N. Wang, Appl. Phys. Lett. **99**, 143112 (2011).
[14] K. Ip, M. E. Overberg, Y. W. Heo, D. P. Norton, S. J. Pearton, C. E. Stutz, B. Luo, F. Ren, D. C. Look, and J. M. Zavada, Appl. Phys. Lett. **82**, 385 (2003).
[15] Y. J. Zeng, Z. Z. Ye, Y. F. Lu, W. Z. Xu, L. P. Zhu, J. Y. Huang, B. He, and Zhao, J. Phys. D: Appl. Phys. **41**, 165104 (2008).
[16] M. Ding, D. X. Zhao, B. Yao, B. H. Li, Z. Z. Zhang, and D. Z. Shen, Appl. Phys. Lett. **98**, 062102 (2011).
[17] K. A. Alim, V. A. Fonoberov, M. Shamsa, and A. Balandin, J. Appl. Phys. **97**, 124313 (2005).
[18] K. Samanta, P. Bhattacharya, R. S. Katiyar, W. Iwamoto, P. G. Pagliuso, and C. Rettori, Phys. Rev. B **73**, 245213 (2006).
[19] B. H. Bairamov, A. Heinrich, G. Irmer, V. V. Toporov, and E. Ziegler, Phys. Status Solidi B **119**, 227 (1983).
[20] R. Cuscó, E. Alarcón-Lladó, L. Artús, J. Ibáñez, J. Jiménez, B. Wang, and M. Callahan, J. Phys. Rev. B **75**, 165202 (2007).
[21] N. Ashkenov, B. N. Mbenkum, C. Bundesmann, V. Riede, and M. Lorenz, J. Appl. Phys. **93**, 126 (2003).
[22] A. Kaschner, U. Haboeck, M. Strassburg, M. Strassburg, and G. Kaczmarczyk, Appl. Phys. Lett. **80**, 1909 (2002).
[23] J. G. Yu, H. Z. Xing, Q. Zhao, H. B. Mao, Y. Shen, J. Q. Wang, Z. S. Lai, and Z. Q. Zhu, Solid State Commun. **138**, 502 (2006).
[24] B. N. Mavrin, L. N. Demyanets, and R. M. Zakalukin, Phys. Rev. A **374**, 4054 (2010).
[25] L. Artús, R. Cuscó, E. Alarcón-Lladó, I. Mártil, G. González-Díaz, J. Jiménez, B. Wang, and M. Callahan, Appl. Phys. Lett. **90**, 181911 (2007).
[26] J. Serrano, A. H. Romero, F. J. Mahjón, R. Lauck, M. Cardona, and A. Rubio, Phys. Rev. B **69**, 094306 (2004).
[27] A. Hoffmann, A. Karschner, and C. Thomsen, Phys. Status Solidi C **0**, 1783 (2003).
[28] C. Kittel, Introduction to Solid State Physics, 8th edn. (John Wiley & Sons, Hoboken, 2005), p. 494.
[29] K. B. Sundaram and A. Khan, J. Vac. Sci. Technol. A **15**, 428 (1997).

